RESEARCH PAPER

Real-time sensors for live monitoring of disease and drug analysis in microfluidic model of proximal tubule

Arun Asif[1] · Kyung Hwan Kim[1] · Faiza Jabbar[1] · Sejoong Kim[2] · Kyung Hyun Choi[1]

Abstract

The quest to replace animal models used in drug testing owing to their lack of accuracy in reflecting human physiology, and the higher comparative cost and time involved in testing with such animal models has given rise to the organ-on-a-chip technology. Organ-on-a-chip-based microphysiological systems are flexible and can be engineered to specifically mimic desired organs and tissue types for the drug discovery and development process. Kidney-specific and non-specific drugs either directly or indirectly affect the kidneys' function by inducing kidney injury. It is quite challenging to integrate electrochemical sensors in the microphysiological systems for continuous monitoring of micro-environment metabolism. We present a theranostic proximal tubule-on-a-chip model for live monitoring of cellular growth pattern. The sensors monitored real-time changes under disease condition and drug treatment based upon cell adhesion and culture medium pH. A glass-based microfluidic chip was designed with integrated transparent electrodes for transepithelial electrical resistance (TEER) monitoring. Additionally, an optical pH sensor and a microscope have been added in the platform for the real-time monitoring of the tissue. This model has the potential to study the absorption and metabolism of the drug along with the capacity to complete and optimize its toxicity assessment.

Keywords Organ on a chip · Nephrotoxicity · Microfluidic · Sensors · Live monitoring

1 Introduction

Recently emerging organ-on-a-chip (OOC)-based bio-microfluidic technologies bear the potential to revolutionize drug testing by minimizing, if not replacing, the usage of animal models. The OOC technology has evolved from the earlier attempts of cell culture integration with microfluidics to the development of multiorgan-on-a-chip -based microphysiological systems (MPSs) (Huh et al. 2010; Sontheimer-Phelps

✉ Sejoong Kim
  sejoong@snubh.org

✉ Kyung Hyun Choi
  amm@jejunu.ac.kr

1 Department of Mechatronics Engineering, Jeju National University, Jeju-si, Jeju-do 63243, Republic of Korea

2 Department of Internal Medicine, Seoul National University Bundang Hospital, Seongnam-si, Gyeonggi-do, Republic of Korea

et al. 2019). From a biological perspective, OOC has matured from cell line cultures to primary cell cultures, and advanced to the development of spheroids and organoids on a chip (Park et al. 2019). Recently, the pharmaceutical industry has shown a decline in research and development productivity due to an increased ratio of failures (Peck et al. 2015). On average, the success rate for drug development has been reduced to 10% of all proposed drugs over the past decade, which has incurred huge financial loss for pharma companies. Owing to higher failure rate, the developmental cost per single FDA approved drug has escalated to 2.6 billion US dollars (Smietana et al. 2016). A key target of OOC technology is to eliminate the unsuccessful drug candidates at the earliest possible stage to reduce the development time and cost.

Commonly prevailing chronic diseases mainly, diabetes, obesity, and hypertension put stress on the kidney's function (Bidani et al. 2013). Over time, the kidney's function is impaired under the influence of diabetes and hypertension (McCallum et al. 2019). The continuous albuminuria (Fig. 1a) develops cellular stress, leading to proximal tubulopathy caused by the progression of inflammation

Fig. 1 a Proximal tubulopathy. Cell injury caused by hyperglycemia leads to renal nephrotoxicity. **b** A schematic representation of the proximal tubule-on-a-chip model
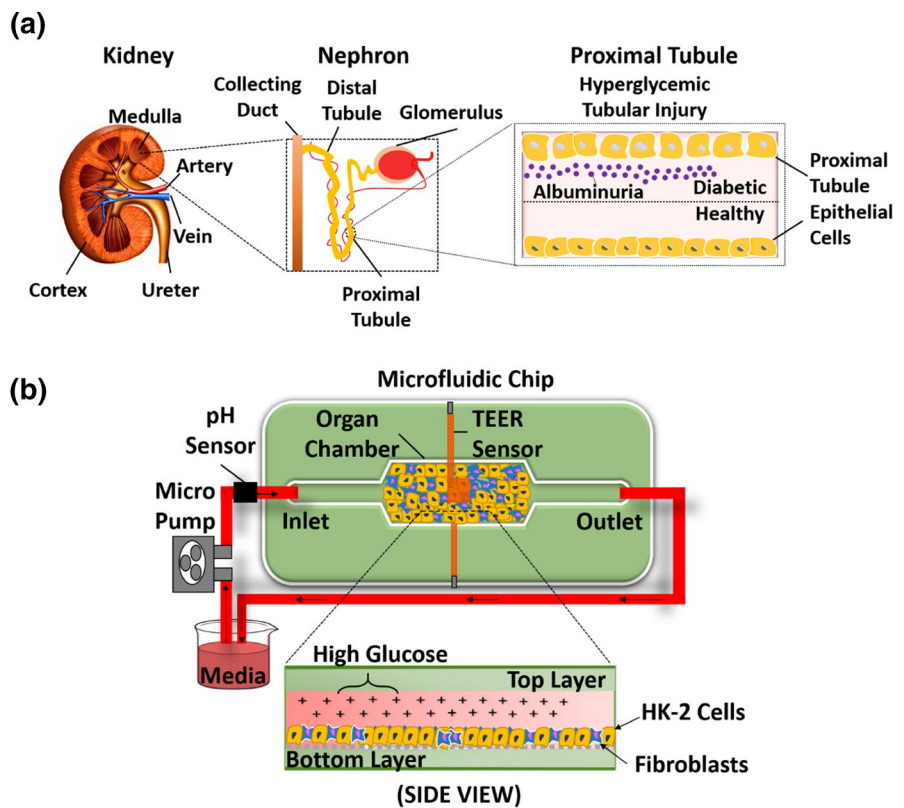
(Gilbert 2017). In normal human physiology, shear stress is an important feature particularly in proximity to stationary phases (Sung et al. 2013). Shear stress promotes physiological changes in tissue through several diverse mechanosensory mechanisms which is absent in 2D cell culture (Kwak et al. 2014). Shear stress has also been shown to affect cell attachment and pathological responses (Califano and Reinhart-King 2010; Meghani et al. 2020). The OOC model of renal nephrotoxicity is considered the most suitable model to mimic kidney physiology for the purpose of drug screening, yet the lack of real-time monitoring is one of the biggest challenges in OOC technology (Kimura et al. 2018).

TEER measurement is a label-free technique to characterize qualitatively the barrier function of the cell monolayer by measuring the resistance across the barrier using the electrodes. The monitoring of tight junctions during the formation of the monolayer of epithelial cells to assess the paracellular permeability can be performed by TEER measurement (Ferrell et al. 2010). Previously, for TEER measurement in a microfluidic chip, metal wires have been integrated above and below the monolayers of the epithelial cells (Douville et al. 2010; van der Helm et al. 2016), cell culture chambers were fabricated between two large electrodes (Vogel et al. 2011), or an electrode assembly on a glass is inserted in a culture device (Yeste et al. 2016). Aforementioned approaches have been found to have variance at large scale. In spite of recent successful integration of gold electrodes

and multi-electrode array with culture chamber construction simultaneously for real-time TEER measurements to monitor the epithelial barrier function (Henry et al. 2017; Maoz et al. 2017), the challenge of live imaging persisted. Moreover, culture media pH is also an important factor to monitor cell growth. Higher level of necrosis and apoptosis of cells in correlation with aggravated cellular stress is associated with decreased pH (Dascalu and Peer 1994). Recently developed kidney OOC systems have implemented kidney proximal tubular cell lines (Duan et al. 2008; Essig et al. 2001), primary proximal tubular cells (Ng et al. 2013), and collecting duct cells (Jang and Suh 2010). With the integration of optical and electrochemical sensors, the cellular growth pattern can be monitored in microfluidic chips to better understand the organ physiology and drug efficacy (Huang and Mason 2013; Soomro et al. 2020; Xu et al. 2019; Zhang et al. 2017).

In the current study, we have designed a proximal tubule-on-a-chip (PTOC) model representing a potential to mimic glucose-induced cytotoxicity in the proximal tubule with integrated sensors. The designed platform facilitates real-time monitoring of TEER and pH values for the first time in a PTOC model. Additionally, a movable microscope is present in platform to continuously observe the cell growth. Indium tin oxide (ITO) was used to print transparent electrodes to facilitate the real-time imaging through integrated microscope. Figure 1b shows a schematic representation of our PTOC platform. Concurrently, the real-time monitoring

via this platform is equally effective for drug efficacy assessment. This kidney model has the potential to be used in the analysis of the initial absorption, excretion, and the toxicology of both kidney-specific drugs and other drugs that may indirectly cause nephrotoxicity.

2 Materials and methods

2.1 Chip fabrication and platform design

A glass-based chip was designed. Two sodalime glasses of 56 mm length and 41 mm width with a thickness of 1.1 mm were used to make a microfluidic chip. Silicon elastomer (Musil medical grade silicon MED-6033) was printed [900 μm width and 200 μm height (h)] using a 3D inkjet printer, figure S1 (Online Resource), to create the microchannel and cell culture chamber on the chip. The width of microchannel was 3 mm and cell culture chamber dimensions were 9 mm width and 20 mm length making 180 mm^2 area.

To establish a TEER sensor on the glass chip, a square-shaped ITO electrodes were printed in the center of the cell culture chamber comprising of 4 mm length (500 nm thickness). The ITO was printed on the glass using a screen-printing technique. The area of one ITO-based TEER electrode was 16 mm^2. The impedance measurements were taken in Ohms (Ω mm^2). A software based on LabVIEW was utilized for monitoring the impedance change from the TEER sensor. Both the glasses were fixed in the chip holder at a position such that the ITO electrodes were placed across one another to complete the circuit to measure electrical resistance. The TEER sensor was calibrated for the characterization of the frequency to monitor the impedance at a fixed frequency. A fixed frequency was derived after evaluating the impedance changes at a frequency range of 1–10,000. The impedance calibration was carried out with Arduino microcontroller by providing a 0.1-V AC potential. The TEER sensor was characterized for different parameters which included media flow, media flow with collagen coating in the cell culture chamber without HK-2 cells, media flow with the collagen coating in the cell culture chamber with HK-2 cell growth on it. The media flow rate did not express a significant influence over the impedance values. The frequency for the continuous monitoring of impedance of the cell culture was optimized at 58.7 Hz. The characterization graph for TEER frequency selection has been provided in figure S2(a) (Online Resource).

To observe the cell growth in real time through a transparent ITO-based TEER sensor, a portable microscope was developed. The microscope assembly comprised of a SCMOS series USB2.0 eyepiece camera (ToupTek™), a lens with 10X magnification power (Plan Achromatic Objective, AmScope™), and a light source (white LED) as shown in figure S3 (Online Resource). A blue wavelength 469 ± 17.5 nm filter was used. ToupView (ToupTek ™) camera control software was used for the high-speed visualization of the images and for video processing.

Additionally, a sensor was established for continuous cell culture media pH measurements. A white LED was employed in a 3D-printed assembly with an optical filter and a photodiode. The pH measurement was based on the principle of the change in light intensity as it passes through the media. A transparent tube was embedded in the pH sensor through which media were passed for pH measurement. The sensor was designed to measure the variations in the media color based upon the changes in the red color of phenol due to acidification of the media over time. The optical signal was quantified by an Arduino microcontroller. The calibration of the pH sensor was accomplished by characterizing the RPMI media (cell culture media used in the experiment) samples with a range of pH from 6.0 to 8.0. The calibration curve of the pH sensor has been presented in figure S2 (b) (Online Resource). Media sample with pH 6.00–8.00 were used because the optimum range for pH of human cell lines is 7.2–7.4 pH. With the passage of time, the pH of the media was reducing due to production of CO_2 and secretion of acidic ions, i.e., HCO_3^-, H^+, etc., (Bernhardt et al. 1988; Gross and Hopfer 1999).

A peristaltic pump was attached to the chip to control the continuous circulation of media. To mimic the shear stress present in proximal tubule microenvironment, the media flow rate upon the cell monolayer in the culture chamber was calibrated. The whole setup of microfluidic platform has been shown in Figure S4 (Online Resource). The in vivo fluid shear stress in proximal tubule microphysiology has previously been characterized as 5 Dyne/cm^2 (Essig and Friedlander 2003). The media flow rate was regulated at 60 μl/min to maintain the 5 Dyne/cm^2 shear stress upon the monolayer of proximal tubule cells. The media shear stress induced in the microchannel of the designed chip was calculated by the use of following equation (Vormann et al. 2018);

$$\tau = \frac{6\mu Q}{wh^2}.$$

Here, "μ" signifies viscosity of the cell culture medium, "Q" exhibits the flow rate of the media, "w" represents the width and height of channel is characterized by "h".

Right behind the media inlet on the chip, an optical pH sensor was attached to the transparent media tube for the real-time pH measurement. Connectors were fixed upon the glass chip by the use of epoxy raisin for connecting the tubes for culture media circulation. The circulation of cell

Fig. 2 The CAD schematic representation of experimental setup. In the inset, an exploded view of the chip has been represented to show the microfluidic channels in the chip
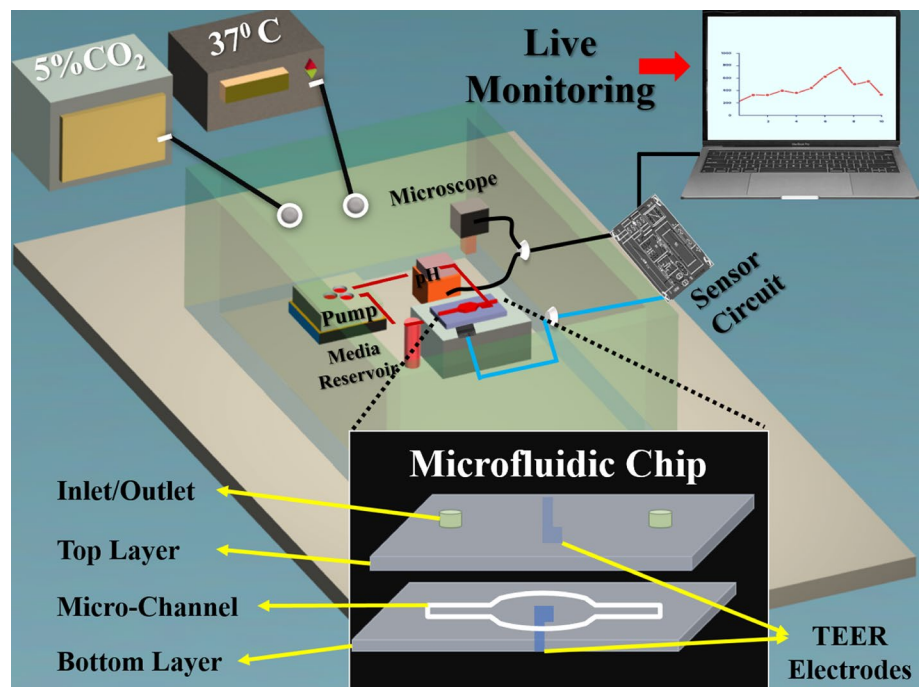
culture media was assisted by a peristaltic pump. Figure 2 represents the experimental setup of the platform assembly. The experiment was performed in triplicate.

2.2 Cell culture

A human-derived kidney tissue cell line of immortalized proximal tubule epithelial cells HK-2 (ATCC®, USA) and human dermal fibroblast cell line CCD-986sk (Korean Cell Line Bank, Republic of Korea) were used to create a coculture model of proximal tubule epithelial cells and fibroblasts. Both the cell lines were grown in RPMI-1640 with 10% fetal bovine serum (FBS) and 1% penicillin and streptomycin, with 5% CO_2 at 37 °C inside the incubator. The cells were cultured in a petri dish until 80–90% confluency was achieved. The cell culture chamber was coated with collagen type I (Sigma-Aldrich™) before cell seeding to facilitate the adhesion of cells onto the ITO-coated glass. Kidney cells (HK-2) and fibroblasts were equally mixed for seeding at an amount of 1×10^5 per ml. The bottom layer of the chip was incubated for 4 h inside the incubator to permit the attachment of the cells. Subsequently, the top layer was fixed upon the bottom layer to complete the microfluidic chip. The chip was attached to a peristaltic micropump on the platform to begin the experiment.

Initially, cells were cultured in normal media (NM) to develop a monolayer of fibroblasts and HK-2 cells for 5 days. Subsequently, a hyperglycemic renal nephrotoxicity model was developed by inducing inflammation in the cells by the usage of high glucose media (HG). It took

3–5 days for the development of inflammation in the monolayer. Next, drug containing media (DM) was circulated for 5 days to assess the efficacy of the drug in reducing the level of inflammation. Commercially available anti-inflammatory drug metformin (Sigma-Aldrich) at a concentration of 5 mM was administered after creating a renal nephrotoxicity model to monitor the cell growth pattern.

The media flow rate was maintained at 60 µl/min. The use of fluid flow within the OOCs of the proximal tubular cell line improves functionality, with studies demonstrating in vivo drug toxicity and pathophysiology. A high glucose media was prepared, containing 25-mM glucose using an anhydrous alpha-D-glucose. Drug containing media were prepared using 10-mM metformin. Metformin hydrochloride (1,1-dimethylbiguanide hydrochloride) was purchased from Sigma-Aldrich®.

2.3 Cells' viability assessment

The Live–Dead Viability/Cytotoxicity Assay Kit® (Invitrogen™, USA) was used as per the provided protocol to assess cell viability. Ethidium homodimer-I (Eth-D) and calcein-AM dyes are used to assess the cell viability; Calcein-A dye is retained by live cells and displays a green fluorescence (ex/em ~ 495 nm/ ~ 515 nm); while, Eth-D penetrates into dead cells to exhibit a red fluorescence (ex/em ~ 495 nm/ ~ 635 nm). Images were captured using a confocal microscope (Olympus FV1200).

2.4 Enzyme-linked immunosorbent assay (ELISA)

The quantification of heat shock protein (HSP70) and kidney injury molecule (KIM-1) was measured using the ELISA assay. HSP70 (Invitrogen) ELISA and KIM-1 (abcam) were performed according to the manufacturers protocol. Optical density was measured using a 450-nm wavelength with a multi-mode microplate reader (Spectra Max i3X).

3 Results and discussion

Kidney function impairment is accompanied by commonly predominant chronic diseases including hypertension and diabetes. High serum glucose induces cytotoxicity with the passage of time due to the development of albuminuria in the proximal tubule, which causes proximal tubulopathy (Gilbert 2017).

The fabrication materials, including ITO for electrode printing and silicone gel for channel printing, were completely biocompatible for cell culture conditions in microfluidic glass chip (Cabal et al. 2014; Moore et al. 2009; Russo et al. 2016). Polydimethylsiloxane (PDMS) has become a mainstream material for chip fabrication owing to its flexibility, permeability and biocompatibility (Ochs et al. 2014). Apart from the merits of PDMS, several disadvantages make it an unsuitable material to analyze cellular metabolism and drugs toxicity. Due to the porosity of PDMS, it becomes permeable for gases and water vapors, and affects the absorption and desorption of drugs (Takano et al. 2014). Additionally, PDMS formation takes place by the crosslinking of toxic oligomers which are released in the cell culture media over the passage of time (Bunge et al. 2018). The glass-based chip was preferred to make this proximal tubule model to eliminate the chances of molecular absorption in the microfluidic channels (Hirama et al. 2019).

3.1 Development of a monolayer of proximal tubule and fibroblast co-culture

First, HK2 and fibroblast cell lines were cultured in NM for 5 days to develop a complete monolayer which was considered equivalent to a proximal tubule tissue. In Fig. 3a, the TEER graph shows an increasing pattern impedance in comparison to control over time until the formation of a complete monolayer of proximal tubule cell line. The impedance value increased exponentially from day 2 until day 4. Due to exponential increase in impedance, a linear graph was obtained before a stability of impedance was achieved on day 5. The exponential increase in the impedance of the cell culture chamber depicts the rapid division of the cells. Once the confluency was achieved, at an elapsed time of 100 h–120 h (day 5) from the beginning of the experiment,

static impedance values were observed. In Fig. 3d, the pH graph exhibits an insignificant decrease of pH in NM as compared to HG and DM.

## 3.2 Nephrotoxicity development by inducing inflammation

Second, NM was replaced with serum-free high glucose media to induce nephrotoxicity. The TEER graph in Fig. 3b shows a decreasing pattern of impedance over time, indicating that tight junctions were decreased. Static impedance values were observed on day 5 of the high glucose exposure indicating that no further tight junctions were breaking apart. The cells were assumed to have developed a nephrotoxic state. The TEER values indicated that the tight junctions decreased drastically from day 2 until day 4 of the high glucose exposure, after which the impedance value stabilized. Figure 3d shows a rapid decline in the pH of the HG media, which represents higher acidity caused by hyperglycemic cell injury during the treatment with high glucose media.

The development of a continuous acidic environment may be linked with the inflammation of cells (Riemann et al. 2015). The magnitude of the pH decrease was noted as being reduced due to the onset of nephrotoxicity leading to cell injury. The impedance and pH change became insignificant on day 5 of high glucose treatment, after which, the drug was administered. As a final step, the drug was passed through the chip to reduce cytotoxicity.

3.3 Drug administration

Figure 3c represents the impedance change in the chip while the drug is administered. It can be clearly seen that because of the drug, the tight junctions among the cells were restored. Although the tight junctions were not restored to the level seen during normal conditions, the restoration was significant enough to demonstrate the difference in cell growth. The TEER measurement revealed significantly important data that can be used to interpret the pattern of cell growth. Similarly, Fig. 3d represents a decline in the pH of the media while undergoing treatment with the drug. The decrease of media pH during drug treatment was noted to be less than the pH decreased under the influence of high glucose. A comparative difference in the pH between its value in the presence of high glucose media and its value in the presence of drug-containing media indicates that the administration of the drug reduced the level of inflammation in the nephrotoxic kidney model. Images taken from the platform integrated microscope are shown in Fig. 4b which represent a monolayer after 5 days of normal cell growth, the cells in the presence of high glucose for 5 days, and the cells after 5-day exposure to drug. Cell culture images were also taken from an inverted light microscope to validate the results of

Fig. 3 Comparative analysis of results. **a** Impedance of the chip in NM from day 1 of the experiment up until the full confluency of the cells is achieved. **b** The impedance of the cells from the point of introduction of HG until the development of nephrotoxicity. **c** The impedance of the cells from the day 1 of DM administration until the stability of the impedance is achieved. **d** pH measurements, a comparative pH graph of the NM, HG and DM from the day 1 up until the day 5. **e** Cell viability assay, average viability count under NM, HG and DM. F. HSP70 and KIM-1 ELISA Assay
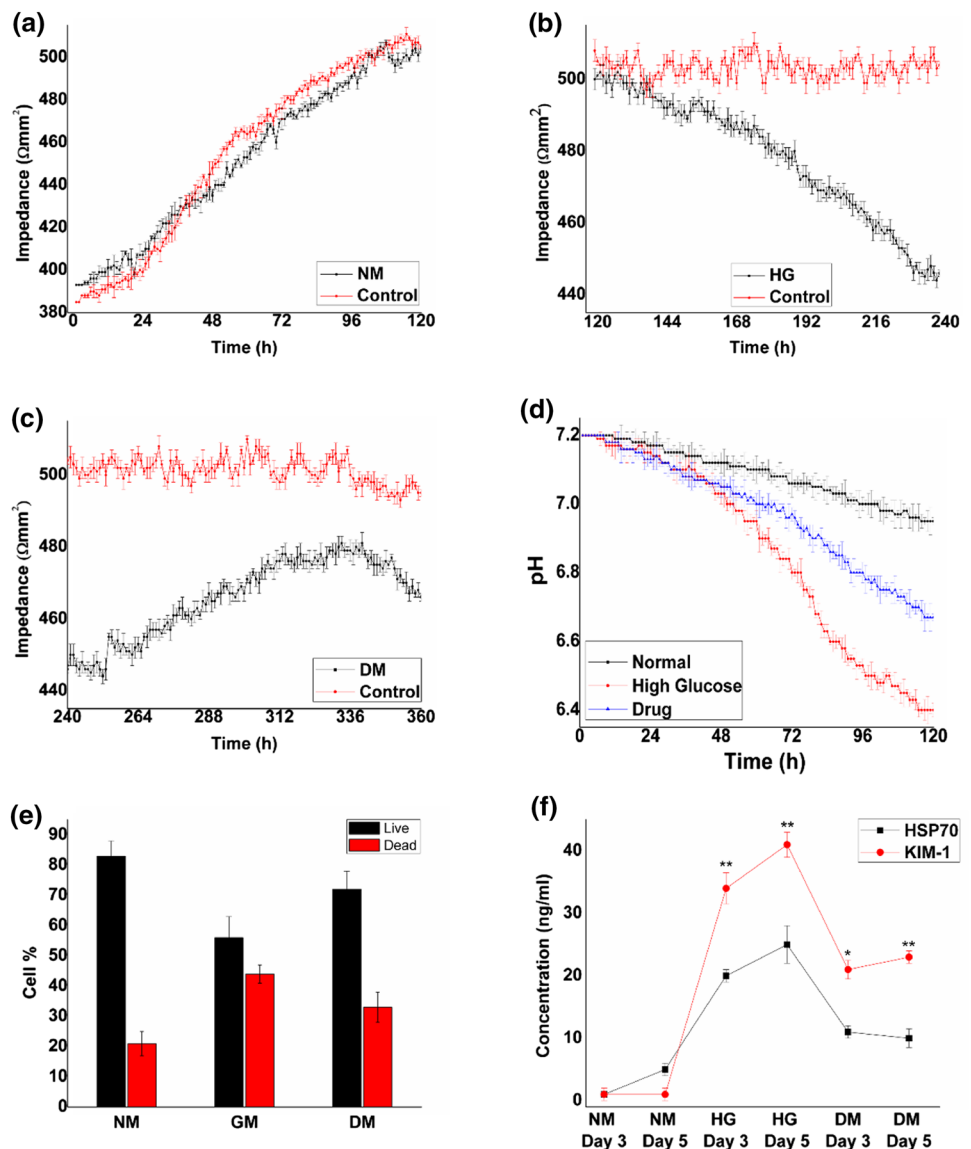
the platform integrated microscope. Images were taken at three intervals during each phase of the experiment. Figure 4a represents the formation of the monolayer in the first phase of the experiment, then the development of inflammation under the influence of high glucose, and the cellular response to the administration of the drug.
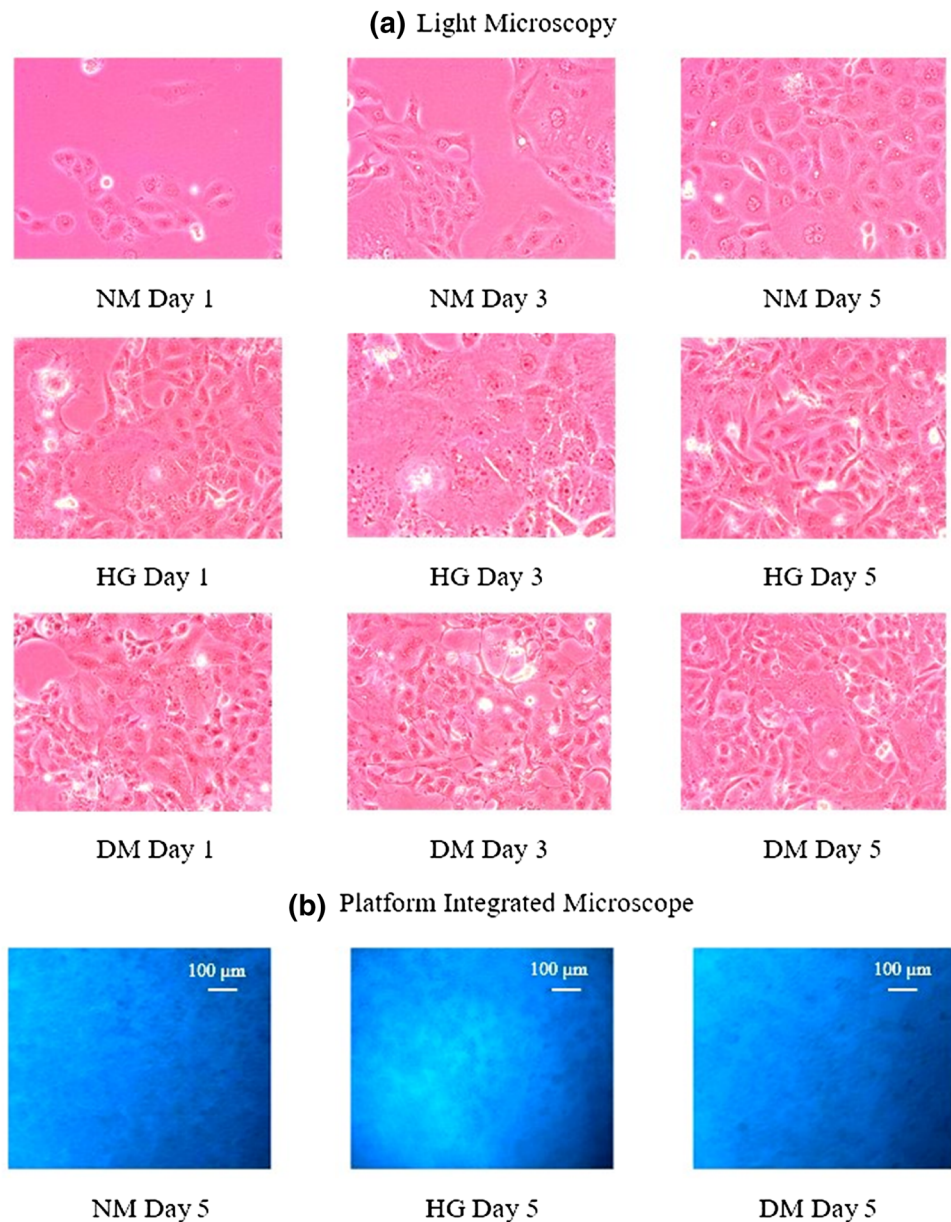
3.4 Live/dead assay

Live/dead assay confocal microscopy images (calcien-AM for live cells, and Eth-D for dead cells) have been depicted in the Fig. 5. Images were analyzed by the use of ImageJ (NIH, USA) software to calculate the percentage of cells. The average viability count fell in a range above 80% in NM. In case of HG exposure for 5 days, the viability reduced to an average below 60%, and after treatment with DM for

5 days, the viability range increased up to 70% of viability, as illustrated in Fig. 3f.

3.5 KIM-1 and HSP70 assay

The comparative cytotoxicity of PTOC based upon the different media types was assessed by the HSP70 and KIM-1 concentration as represented in Fig. 6. A higher secretion of HSP70 and KIM-1 was linked to inflammation, which was considered a suitable model for kidney nephrotoxicity for subsequent drug testing (Van Eden et al. 2007). The HSP70 and KIM-1 release with NM culture was recorded to be insignificant. A significant quantity of both the biomarkers was recorded on day 3 and day 5 of HG administration. KIM-1 was found to be more significant in the media ranging from 30 to 40 ng/ml as compared to HSP70 which represent a 20–25 ng/ml.

Fig. 4 a The inverted micro-
scope images of the HK2 cells
and Fibroblasts. NM represents
normal media until conflu-
ency is attained. HG represents
high-glucose media and DM
represents treatment with an
anti-inflammatory drug. (All
the images were taken at 100X
magnification.) **b** Microscopic
Images from platform integrated
microscope. Cells after 5 days
of incubation with NM, HG and
DM, respectively (scale bar is
100 μm)

(a) Light Microscopy

NM Day 1 — NM Day 3 — NM Day 5

HG Day 1 — HG Day 3 — HG Day 5

DM Day 1 — DM Day 3 — DM Day 5

(b) Platform Integrated Microscope

NM Day 5 — HG Day 5 — DM Day 5

In comparison with HG day 3, the day 5 value of both biomarkers exhibited a 20% increase in their concentrations indicating a higher cellular stress and necrosis. Once the diseased condition was created after 5 days of high glucose exposure, the DM was applied. The cellular stress was found to be reduced at a rate of 50% within 3 days of DM exposure. A steady subsequent value of the biomarkers was measured on day 5 under drug administration. The ELISA assay further validated the data collected using TEER and pH sensor.

The current PTOC model presents an outlook for the real-time monitoring of cell growth. In Figure S5 and Figure S6 (Online Resource), a spectrum of collective impedance values and pH values represented throughout the experiment is shown, respectively, which correlates with ELISA assay and live/dead results. The average impedance values from the TEER sensor expressed a surge in resistance over the course of the monolayer formation. The impedance values were found to be following the exact pattern of the cell growth. A similar trend was observed in the collective spectra of pH values over the duration of monolayer formation in the experiment.

The PTOC model exhibited an increased level of cellular toxicity leading to cell injury under HG culture. TEER and pH sensors continuously monitored the inflammation over a period of 5 days. The pattern of pH variation over time (Fig. 3d) indicates that under the influence of HG most significant level of pH decrease was measured, indicating extreme cell toxicity due to the high-glucose media. Simultaneously, the HSP70

(a) Normal Media

(b) High Glucose Media

(c) Media with Drug
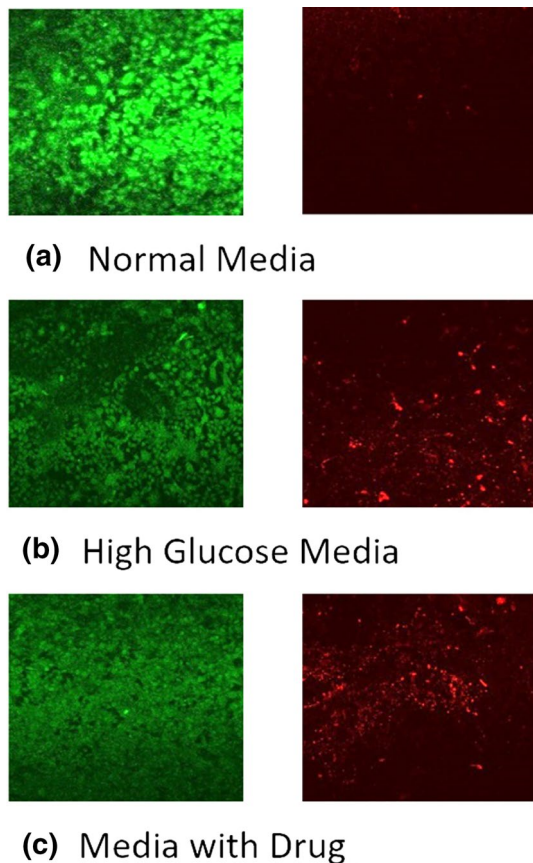
Fig. 5 Representative confocal microscopy images for live/dead assay of proximal tubule-on-a-chip model
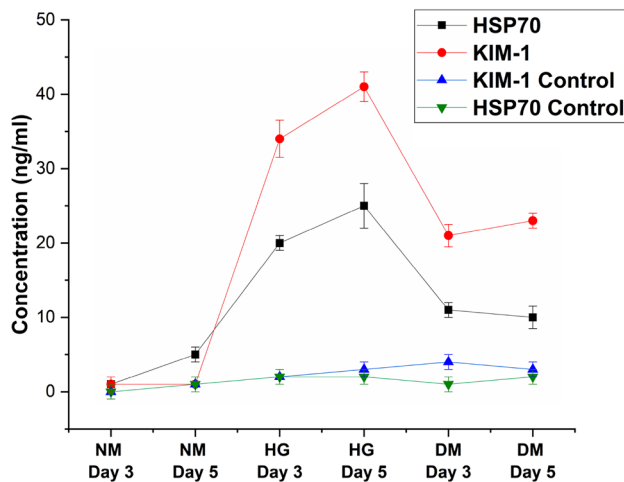
Fig. 6 The ELISA assay results of the HSP70 and KIM-1 biomarkers. Serum samples were collected on day 3 and day 5 of cellular growth with NM, HG and DM. All values are represented as mean ± SEM, $n = 3$ in each group. *, **, ***Represent statistical significance from control in graph A and B, and statistical significance of KIM-1 over HSP70 in Fig. 3f at $p < 0.05$, $p < 0.01$ and $p < 0.001$, respectively

and KIM-1 results expressed a rise in HSP70 concentration indicating a higher level of inflammation.

Subsequently, for drug efficacy assessment, the anti-inflammatory drug was administered to monitor the PTOC response towards drug. The cell growth under DM represented a decline in pH which can be observed in the Fig. 3d. Drug treatment reduced the cellular toxicity due to which the decline of the pH was relatively less as compared to the corresponding values in the presence of high glucose media.

Owing to the results of TEER and pH sensors validated by HSP70 and KIM-1 ELISA assay and Live/dead assay images, we infer that the TEER and pH sensors are equally reliable. The current TEER monitoring system is advantageous due to simultaneous imaging capability. The integrated microscope captured real-time images correlated with TEER results. The comparative reliability of the sensors with respect to the conventional biological assays validates the live monitoring offered by our OOC platform.

In recent past, a few proximal tubule microfluidic models have been developed with the capacity to mimic both normal and diseased condition of the proximal tubule cells; however, PDMS was implemented for fabrication material in these chips (Jang et al. 2013; Sakolish et al. 2019; Vormann et al. 2018; Vriend et al. 2020). Here, we present a unique PTOC model with a glass-based chip for the first time with integrated optical and electrochemical sensors. The glasses chip is a perfect candidate for the electrode printing without distorting the surface for cell culture. The results from the current study demonstrated a successful execution of the mimicking of proximal tubule with live monitoring by sensors of the designed PTOC model. It has potential to advance the field of bio-microfluidics for evaluating the real-time changes in human tissue microphysiology. From the correlation of TEER and pH sensor in the PTOC model, it can be inferred that both these parameters are closely correlated with the cell growth pattern. Currently, the PTOC model has been developed by the use of cell lines and represents only the proximal tubular part of the nephron. In future, the OOC platform will be upgraded to incorporate primary cells, a multichambered chip to represent more than one part of the organ and more physiological sensors to monitor the growth in a precise manner. The real-time monitoring of the continuously changing media conditions caused by cellular growth under the influence of different toxic agents makes the PTOC model a suitable platform for drug toxicity assessment.

4 Conclusion

Our work represents a robust method for the live monitoring of PTOC model through a TEER sensor, and a pH sensor along with real-time microscopy. The platform successfully

monitored continuous TEER and pH values with the integrated sensors exhibiting cell injury and drug efficacy. We conclude that our PTOC model assesses the nephrotoxicity and efficacy of potential drugs candidates at the initial stage of drug development. The platform is cost effective owing to its rapid disease development and monitoring capabilities in limited timeframe and offers an improved correlation with human clinical conditions. In the future, this platform can be designed to have a better capacity to incorporate complex multilayer chip models and can operate multiple chips simultaneously to mimic the nephron physiology including all four chambers.

Compliance with ethical standards

Conflict of interest The authors declare no conflict of interest.

References

Bernhardt G, Distèche A, Jaenicke R, Koch B, Lüdemann H-D, Stetter K-O (1988) Effect of carbon dioxide and hydrostatic pressure on the pH of culture media and the growth of methanogens at elevated temperature. Appl Microbiol Biotechnol 28:176–181

Bidani AK, Polichnowski AJ, Loutzenhiser R, Griffin KA (2013) Renal microvascular dysfunction, hypertension and CKD progression. Curr Opin Nephrol Hypertens 22:1

Bunge F, van den Driesche S, Vellekoop MJ (2018) PDMS-free microfluidic cell culture with integrated gas supply through a porous membrane of anodized aluminum oxide. Biomed Microdevices 20:98

Cabal B, Alou L, Cafini F, Couceiro R, Sevillano D, Esteban-Tejeda L, Guitián F, Torrecillas R, Moya JS (2014) A new biocompatible and antibacterial phosphate free glass-ceramic for medical applications. Sci Rep 4:5440

Califano JP, Reinhart-King CA (2010) Exogenous and endogenous force regulation of endothelial cell behavior. J Biomech 43:79–86

Dascalu A, Peer A (1994) Effects of radiologic contrast media on human endothelial and kidney cell lines: intracellular pH and cytotoxicity. Acad Radiol 1:145–150

Douville NJ, Tung Y-C, Li R, Wang JD, El-Sayed ME, Takayama S (2010) Fabrication of two-layered channel system with embedded electrodes to measure resistance across epithelial and endothelial barriers. Anal Chem 82:2505–2511

Duan Y, Gotoh N, Yan Q, Du Z, Weinstein AM, Wang T, Weinbaum S (2008) Shear-induced reorganization of renal proximal tubule cell actin cytoskeleton and apical junctional complexes. Proc Natl Acad Sci 105:11418–11423

Essig M, Friedlander G (2003) Tubular shear stress and phenotype of renal proximal tubular cells. J Am Soc Nephrol 14:S33–S35

Essig M, Terzi F, Burtin M, Friedlander G (2001) Mechanical strains induced by tubular flow affect the phenotype of proximal tubular cells. Am J Physiol Ren Physiol 281:F751–F762

Ferrell N, Desai RR, Fleischman AJ, Roy S, Humes HD, Fissell WH (2010) A microfluidic bioreactor with integrated transepithelial electrical resistance (TEER) measurement electrodes for evaluation of renal epithelial cells. Biotechnol Bioeng 107:707–716

Gilbert RE (2017) Proximal tubulopathy: prime mover and key therapeutic target in diabetic kidney disease. Diabetes 66:791–800. https://doi.org/10.2337/db16-0796

Gross E, Hopfer UJ (1999) Effects of pH on kinetic parameters of the Na–HCO$_3$ cotransporter in renal proximal tubule. Biophys J 76:3066–3075

Henry OY, Villenave R, Cronce MJ, Leineweber WD, Benz MA, Ingber DE (2017) Organs-on-chips with integrated electrodes for trans-epithelial electrical resistance (TEER) measurements of human epithelial barrier function. Lab Chip 17:2264–2271

Hirama H, Satoh T, Sugiura S, Shin K, Onuki-Nagasaki R, Kanamori T, Inoue T (2019) Glass-based organ-on-a-chip device for restricting small molecular absorption. J Biosci Bioeng 127:641–646

Huang Y, Mason AJ (2013) Lab-on-CMOS integration of microfluidics and electrochemical sensors. Lab Chip 13:3929–3934

Huh D, Matthews BD, Mammoto A, Montoya-Zavala M, Hsin HY, Ingber DE (2010) Reconstituting organ-level lung functions on a chip. Science 328:1662–1668

Jang K-J, Suh K-Y (2010) A multi-layer microfluidic device for efficient culture and analysis of renal tubular cells. Lab Chip 10:36–42

Jang K-J, Mehr AP, Hamilton GA, McPartlin LA, Chung S, Suh K-Y, Ingber DE (2013) Human kidney proximal tubule-on-a-chip for drug transport and nephrotoxicity assessment. Integr Biol 5:1119–1129

Kimura H, Sakai Y, Fujii T (2018) Organ/body-on-a-chip based on microfluidic technology for drug discovery. Drug Metab Pharmacokinet 33:43–48

Kwak BR, Bäck M, Bochaton-Piallat ML, Caligiuri G, Daemen MJ, Davies PF, Hoefer IE, Holvoet P, Jo H, Krams R, Lehoux S (2014) Biomechanical factors in atherosclerosis: mechanisms and clinical implications. Eur Heart J 35:3013–3020d. https://doi.org/10.1093/eurheartj/ehu353

Maoz BM, Herland A, Henry OY, Leineweber WD, Yadid M, Doyle J, Mannix R, Kujala VJ, FitzGerald EA, Parker KK, Ingber DE (2017) Organs-on-Chips with combined multi-electrode array and transepithelial electrical resistance measurement capabilities. Lab Chip 17:2294–2302

McCallum W, Ku E, Sarnak MJ (2019) More evidence to suggest a relation of blood pressure to long-term progression of kidney disease: is it causal? Am J Kidney Dis 74:293–296

Meghani NM, Amin H, Park C, Cui J-H, Cao Q-R, Choi KH, Lee B-J (2020) Combinatory interpretation of protein corona and shear stress for active cancer targeting of bioorthogonally clickable gelatin-oleic nanoparticles. Mater Sci Eng, C 111:110760. https://doi.org/10.1016/j.msec.2020.110760

Moore E, Rawley O, Wood T, Galvin PJS, Chemical AB (2009) Monitoring of cell growth in vitro using biochips packaged with indium tin oxide sensors. Sens Actuators B Chem 139:187–193

Ng CP, Zhuang Y, Lin AWH, Teo JCM (2013) A fibrin-based tissue-engineered renal proximal tubule for bioartificial kidney devices: development, characterization and in vitro transport study. Int J Tissue Eng 2013:319476

Ochs CJ, Kasuya J, Pavesi A, Kamm RD (2014) Oxygen levels in thermoplastic microfluidic devices during cell culture. Lab Chip 14:459–462

Park SE, Georgescu A, Huh D (2019) Organoids-on-a-chip. Science 364:960–965

Peck RW, Lendrem DW, Grant I, Lendrem BC, Isaacs JD (2015) Why is it hard to terminate failing projects in pharmaceutical R&D? Nat Rev Drug Discov 14:663

Riemann A, Ihling A, Thomas J, Schneider B, Thews O, Gekle M (2015) Acidic environment activates inflammatory programs in fibroblasts via a cAMP–MAPK pathway. Biochimica et Biophysica ACTA (BBA) (Molecular Cell Research) 1853:299–307

Russo S, Ranzani T, Walsh C, Wood R (2016) A soft pop-up proprioceptive actuator for minimally invasive surgery. In: The 9th Hamlyn Symposium on Medical Robotics, London, June 25–28, pp. 750–757

Sakolish CM, Philip B, Mahler GJJB (2019) A human proximal tubule-on-a-chip to study renal disease and toxicity. Biomicrofluidics 13:014107

Smietana K, Siatkowski M, Møller M (2016) Trends in clinical success rates. Nat Rev Drug Discov 15:379

Sontheimer-Phelps A, Hassell BA, Ingber DE (2019) Modelling cancer in microfluidic human organs-on-chips. Nat Rev Cancer 19:65–81

Soomro AM, Khalid MAU, Shah I, wan Kim S, Kim YS, Choi KH (2020) Highly stable soft strain sensor based on Gly-KCl filled sinusoidal fluidic channel for wearable and water-proof robotic applications. Smart Mater Struct 29:025011

Sung JH, Esch MB, Prot J-M, Long CJ, Smith A, Hickman JJ, Shuler ML (2013) Microfabricated mammalian organ systems and their integration into models of whole animals and humans. Lab Chip 13:1201–1212

Takano A, Tanaka M, Futai N (2014) On-chip multi-gas incubation for microfluidic cell cultures under hypoxia. Biomicrofluidics 8:061101

van der Helm MW, Odijk M, Frimat J-P, van der Meer AD, Eijkel JC, van den Berg A, Segerink LI (2016) Direct quantification of transendothelial electrical resistance in organs-on-chips. Biosens Bioelectron 85:924–929

Van Eden W, Wick G, Albani S, Cohen I (2007) Stress, heat shock proteins, and autoimmunity: how immune responses to heat shock proteins are to be used for the control of chronic inflammatory diseases. Ann N Y Acad Sci 1113:217–237

Vogel PA, Halpin ST, Martin RS, Spence DM (2011) Microfluidic transendothelial electrical resistance measurement device that enables blood flow and postgrowth experiments. Anal Chem 83:4296–4301

Vormann MK, Gijzen L, Hutter S, Boot L, Nicolas A, van den Heuvel A, Vriend J, Ng CP, Nieskens TT, van Duinen V, de Wagenaar B (2018) Nephrotoxicity and kidney transport assessment on 3D perfused proximal tubules. AAPS J 20:90

Vriend J, Peters JG, Nieskens TT, Škovroňová R, Blaimschein N, Schmidts M, Roepman R, Schirris TJ, Russel FG, Masereeuw R, Wilmer MJ (2020) Flow stimulates drug transport in a human kidney proximal tubule-on-a-chip independent of primary cilia. Biochimica et Biophysica Acta (BBA)-General. Subjects 1864:129433

Xu K, Chen Y, Okhai TA, Snyman LWJ (2019) Micro optical sensors based on avalanching silicon light-emitting devices monolithically integrated on chips. Opt Mater Express 9:3985–3997

Yeste J, Illa X, Gutiérrez C, Solé M, Guimerà A, Villa R (2016) Geometric correction factor for transepithelial electrical resistance measurements in transwell and microfluidic cell cultures. J Phys D Appl Phys 49:375401

Zhang YS, Aleman J, Shin SR, Kilic T, Kim D, Shaegh SA, Massa S, Riahi R, Chae S, Hu N, Avci H (2017) Multisensor-integrated organs-on-chips platform for automated and continual in situ monitoring of organoid behaviors. Proc Natl Acad Sci 114:E2293–E2302